# Binding to Redox-Inactive Alkali and Alkaline Earth Metal Ions Strongly Deactivates the C−H Bonds of Tertiary Amides toward Hydrogen Atom Transfer to Reactive Oxygen Centered Radicals

Michela Salamone, Giulia Carboni, Livia Mangiacapra, and Massimo Bietti*

Dipartimento di Scienze e Tecnologie Chimiche, Università "Tor Vergata", Via della Ricerca Scientifica, 1, I-00133 Rome, Italy

S *Supporting Information*

ABSTRACT: The effect of alkali and alkaline earth metal ions on the reactions of the cumyloxyl radical (CumO$^\bullet$) with N,N-dimethylformamide (DMF) and N,N-dimethylacetamide (DMA) was studied by laser flash photolysis. In acetonitrile, a >2 order of magnitude decrease in the rate constant for hydrogen atom transfer (HAT) from the C−H bonds of these substrates (k_H) was measured after addition of Li$^+$. This behavior was explained in terms of a strong interaction between Li$^+$ and the oxygen atom of both DMF and DMA that increases the extent of positive charge on the amide, leading to C−H bond deactivation toward HAT to the electrophilic radical CumO$^\bullet$. Similar effects were observed after addition of Ca^{2+}, which was shown to strongly bind up to four equivalents of the amide substrates. With Mg^{2+}, weak C−H deactivation was observed for the first two substrate equivalents followed by stronger deactivation for two additional equivalents. No C−H deactivation was observed in DMSO after addition of Li$^+$ and Mg^{2+}. These results point toward the important role played by metal ion Lewis acidity and solvent Lewis basicity, indicating that C−H deactivation can be modulated by varying the nature of the metal cation and solvent and allowing for careful control over the HAT reactivity of amide substrates.
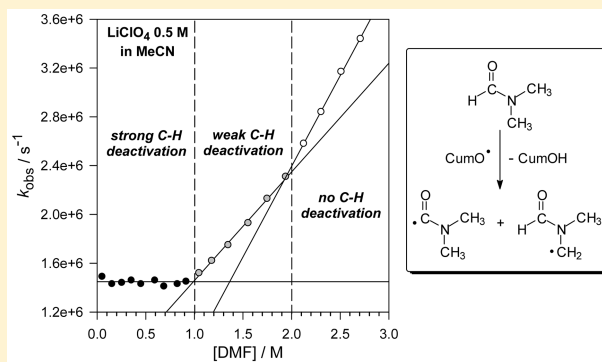
INTRODUCTION

Alkali and alkaline earth metal ions are deeply involved in a variety of biochemical processes, where they have been shown to play both structural and catalytic roles. These metal ions can interact with nucleic acids,[1−3] peptides, and proteins,[4−9] and such interactions can have a strong impact on the structure and function of these biomolecules. Alkali and alkaline earth metal ions are involved, moreover, in a large number of enzymatic reactions,[10,11] and it is also well-established that these ions can play important roles in controlling biological redox reactions. As an example, the redox-inactive metal cation Ca^{2+} is essential for activity in the oxygen-evolving complex (OEC), the cubane-like heteronuclear Mn$_4$CaO$_5$ cluster that is the site of water oxidation in photosystem II (PSII),[12] although its exact role in catalysis remains unclear.[13]

By acting as Lewis acids, redox-inactive alkali, alkaline earth, or transition metal ions have also been shown to play a key role in biomimetic redox reactions. Relevant examples include the promotion of O−O bond cleavage during dioxygen activation at nonheme iron centers,[14,15] the modulation of oxygen release in nonheme iron peroxo complexes,[16] the increase in radical scavenging activity of phenolic antioxidants[17,18] and in electron transfer and oxygen atom transfer reactivity of nonheme metal−oxo complexes,[19] the decrease in the efficiency of hole tranport in DNA,[20] and the modulation of the redox potential of the catalyst in water oxidation reactions catalyzed by transition metal oxide clusters.[21]

Redox-inactive metal ions also have been shown to influence the hydrogen atom abstraction reactivity of metal−oxo complexes. An up to 180-fold decrease in the rate constant (k_H) for hydrogen atom transfer (HAT) from 1,4-cyclohexadiene to Mn(IV)−oxo complexes was measured after binding Sc^{3+},[22] a behavior that was explained on the basis of steric effects as a consequence of the increased hindrance determined by the metal ions bound to the Mn−oxo moiety. An increase in k_H was instead measured after binding of Zn^{2+} to a Mn(IV)−oxo complex[23] and of Sc^{3+} to a Fe(IV)−oxo complex.[24] The opposite reactivity trends observed in these reactions indicate that the effect of metal ions on the hydrogen atom abstraction reactivity of metal−oxo complexes is yet to be clarified, suggesting that, in order to provide a deeper understanding of these effects, additional studies are needed.

Interestingly, in the reactions with a prototypical oxygen centered radical such as cumyloxyl (PhC(CH$_3$)$_2$O$^\bullet$, CumO$^\bullet$), a slight increase in k_H was measured for HAT from 1,4-cyclohexadiene after addition of Li$^+$ or Mg^{2+}.[25] This behavior was rationalized on the basis of the interaction of the metal ion with the radical oxygen atom that, by increasing the electron deficiency at the radical center, determines an increase in its hydrogen atom abstraction reactivity toward C−H bonds. Most importantly, when HAT from the α-C−H bonds of tertiary

aliphatic amines to CumO$^\bullet$ was studied in acetonitrile in the presence of lithium and magnesium salts, a 2-fold decrease in k_H was measured after addition of Li$^+$, whereas only an upper limit to k_H could be determined after addition of Mg^{2+}, showing that the latter metal ion leads to a greater than 2 order of magnitude decrease in k_H.[25] These results point toward the significantly stronger interaction of both Li$^+$ and Mg^{2+} with the substrate as compared to that of CumO$^\bullet$, where the observed kinetic effects were explained in terms of C−H bond deactivation via formation of a Lewis acid−base complex between the metal ion and the amine. It was proposed that this interaction decreases the degree of overlap between the α-C−H σ^* orbital and the heteroatom lone pair, leading to an increase in the strength of this bond and to a corresponding decrease in k_H. Strong support for this picture was recently provided by computational studies, showing that, in the reaction of CumO$^\bullet$ with triethylamine, the interaction between Mg^{2+} and the nitrogen lone pair leads to a 5.1 kcal mol^{-1} increase in the α-C−H bond dissociation energy (BDE) and to a greater than 4 order of magnitude decrease in k_H.[26] Polar contributions to the HAT transition state were also shown to play an important role. It is generally accepted that the transition state for HAT from aliphatic C−H bonds to oxygen centered radicals is characterized by a certain extent of charge separation,[27,28] with the development of negative charge on the radical oxygen atom and positive charge on the incipient carbon centered radical (Scheme 1a, showing the transition state for HAT from

Scheme 1
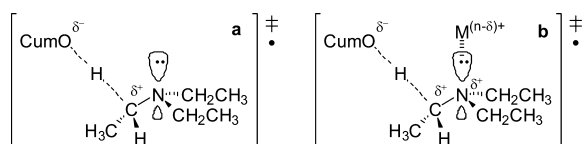
the α-C−H bonds of triethylamine to CumO$^\bullet$). Accordingly, in the reaction of the electrophilic radical CumO$^\bullet$ with amines, metal ion binding will decrease the electron density at the incipient radical center (Scheme 1b, showing the effect of a metal ion M^{n+} on the HAT transition state), leading to a destabilization of the HAT transition state and to a corresponding decrease in k_H.

As pointed out previously,[25] because these effects result from the preferential interaction of the metal ion with the substrate, C−H deactivation should also be observed in the reactions of other electrophilic radicals and hydrogen atom abstracting species with amines and with other substrates characterized by the presence of Lewis basic sites in proximity of the abstractable hydrogen atoms.

Alkanamides are relatively strong Lewis basic substrates,[29] and, accordingly, on the basis of this mechanistic picture, an analogous C−H bond deactivation may also be observed in their reactions with CumO$^\bullet$ following alkali and alkaline earth metal ion addition. This possibility appears to be of great interest in view of the large number of recently described synthetically useful C−H functionalization procedures based on HAT from amides to alkoxyl radicals.[31]

Another aspect of great relevance is represented by the fact that amides are often employed for a variety of purposes as simple models for the peptide bond. Along this line, an understanding of the effect of metal ions on HAT from the C−H bonds of amides may also represent a fundamental starting

point for the study of analogous effects on HAT from the C−H bonds of peptides and proteins to reactive oxygen centered radicals.

In view of these aspects and of the relevance of these reactions and to develop a general understanding of the role of redox-inactive metal ions on HAT reactions from basic substrates to alkoxyl radicals, we have carried out a detailed time-resolved kinetic study in acetonitrile and DMSO solutions on the effect of alkali and alkaline earth metal ion salts (LiClO$_4$, LiOTf, NaClO$_4$, Mg(ClO$_4$)$_2$ and Ca(ClO$_4$)$_2$) on the reactions of CumO$^\bullet$ with N,N-dimethylformamide (DMF) and N,N-dimethylacetamide (DMA). The HAT reactivity and selectivity observed in acetonitrile, in the absence of added salts, for reaction of CumO$^\bullet$ with DMF and DMA has been previously investigated (see below).[32]

■ RESULTS AND DISCUSSION

CumO$^\bullet$ was generated at $T = 25$ °C by 266 or 355 nm laser flash photolysis (LFP) of argon-saturated acetonitrile or DMSO solutions containing dicumyl peroxide (0.01 and 1.0 M, respectively). In these solvents, CumO$^\bullet$ displays a visible absorption band centered at 485 nm and a lifetime in the microsecond time domain that allow the direct measurement of HAT rate constants by LFP.[33,34] In the absence of added substrate, CumO$^\bullet$ decays mainly by C−CH$_3$ β-scission (eq 1),[35] whereas in acetonitrile or DMSO, HAT from the solvent C−H bonds plays a negligible role as a consequence of the operation of deactivating polar effects.[28,35]
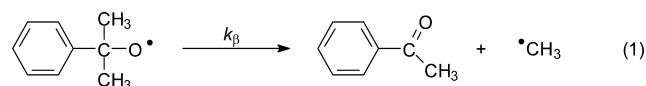
The reactions of CumO$^\bullet$ with DMF and DMA were studied by employing the LFP technique. A time-resolved kinetic study on the reactions of CumO$^\bullet$ with DMF and DMA was recently carried out in acetonitrile solution.[32] Identical rate constants were measured for HAT from the C−H bonds of the two substrates ($k_H = 1.24 \times 10^6$ M^{-1} s^{-1}). With DMF, HAT to CumO$^\bullet$ was shown to occur from both the formyl and N-methyl groups, with the formyl C−H bond being the preferred reactive site. In the reaction with DMA, preferential HAT from the C−H bonds of the N-methyl groups was observed, with HAT from the acetyl group playing a minor role.

k_H values for HAT from DMF and DMA to CumO$^\bullet$ in DMSO solution were measured by 355 nm LFP following the decay of the CumO$^\bullet$ visible absorption band as a function of amide concentration. When the observed rate constants (k_{obs}) were plotted against [amide], excellent linear relationships were observed and the k_H values were obtained from the slope of these plots. The k_{obs} vs [substrate] plots for the reactions of CumO$^\bullet$ with DMF and DMA in DMSO solution at $T = 25$ °C are displayed in the Supporting Information (Figures S1 and S2). The k_H values thus obtained are collected in Table 1, together with the k_H values measured previously for the corresponding reactions carried out in acetonitrile solution.[32,36]

The data collected in Table 1 show that DMF and DMA display very similar rate constants in their reactions with CumO$^\bullet$: $k_H = 2.50 \times 10^6$ and 2.41×10^6 M^{-1} s^{-1}, respectively, values that are about 2 times higher than the corresponding k_H values measured in acetonitrile. A similar behavior was previously observed in the reactions of CumO$^\bullet$ with triethyl-amine and alkanediamines, where k_H was found to increase on

Table 1. Second-Order Rate Constants (k_H) for the Reaction of the Cumyloxyl Radical (CumO[•]) with *N,N*-Dimethylformamide (DMF) and *N,N*-Dimethylacetamide (DMA)

	k_H/M^{-1} s^{-1a}	
	MeCN	DMSO
DMF	$1.24 \pm 0.02 \times 10^{6b,d}$	$2.50 \pm 0.06 \times 10^{6c}$
	$1.32 \pm 0.02 \times 10^{6c,e}$	
DMA	$1.24 \pm 0.03 \times 10^{6b,d}$	$2.41 \pm 0.05 \times 10^{6c}$

[a]Measured in argon-saturated solution at T = 25 °C employing 266 or 355 nm LFP, from the slope of the k_{obs} vs [substrate] plots, where, in turn, k_{obs} values were measured following the decay of the CumO[•] visible absorption band at 490 nm. Average of at least two determinations. [b]266 nm LFP, [dicumyl peroxide] = 0.010 M. [c]355 nm LFP, [dicumyl peroxide] = 1.0 M. [d]Ref 32. [e]Ref 36.

going from acetonitrile to DMSO ($k_{H(DMSO)}/k_{H(MeCN)}$ = 1.3–1.6)[37] and was explained on the basis of the greater hydrogen-bond donor (HBD) ability of MeCN as compared to that of DMSO.[38] The same explanation reasonably accounts for the increase in reactivity observed for DMF and DMA. On the basis of the development of a certain extent of charge separation in the transition state for HAT from aliphatic C–H bonds to CumO[•] discussed above and displayed in Scheme 1 for the reaction of triethylamine, solvent hydrogen bonding will decrease the electron density at the incipient radical center with both amine and amide substrates (Scheme 2, showing the effect

Scheme 2
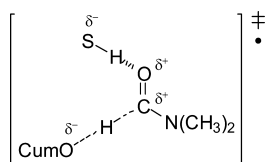
of an HBD solvent SH on the transition state for HAT from the formylic C–H bond of DMF to CumO[•]), leading to a destabilization of the HAT transition state and to a corresponding decrease in k_H as compared to non-HBD solvents.[35]

The effect of alkali and alkaline earth metal ions on the HAT reactivity of DMF and DMA toward CumO[•] was then investigated. The following metal ion salts were employed in acetonitrile solution: LiClO$_4$, LiOTf, NaClO$_4$, Mg(ClO$_4$)$_2$, and Ca(ClO$_4$)$_2$. In DMSO, the study was limited to LiClO$_4$ and Mg(ClO$_4$)$_2$. The time-resolved kinetic studies were carried out by LFP at a constant salt concentration (between 0.2 and 1.0 M) by following the decay of the CumO[•] visible absorption band at 490 nm as a function of the amide concentration. Previous studies have clearly shown the stability of dicumyl peroxide to metal ion salts under the experimental conditions employed.[25]

Figure 1a,b shows the plots of k_{obs} vs [substrate] for the reactions of CumO[•] with DMF and DMA in acetonitrile containing 0.5 and 0.2 M LiClO$_4$, respectively. Concerning DMF, no significant increase in k_{obs} was observed up to [DMF] = 1.0 M (Figure 1a, black circles). A linear increase in k_{obs} with increasing [DMF] was observed in the 1.0–2.0 M concentration range (Figure 1a, gray circles) and above this concentration and with a different slope up to [DMF] = 2.7 M (Figure 1a, white circles). The HAT rate constants were obtained from the slope of the plots in the 1.0–2.0 and 2.0–2.7 M ranges as k_{H1} = 8.91 × 10^5 M^{-1} s^{-1} and k_{H2} = 1.49 × 10^6 M^{-1} s^{-1}, respectively.

An analogous behavior was observed when the reaction of CumO[•] with DMF was carried out in the presence of 0.2 and 1.0 M LiClO$_4$ and when employing 266 nm LFP for CumO[•] generation (Figure S3).

With DMA, no significant increase in k_{obs} was observed up to [DMA] = 0.2 M (Figure 1b, black circles). A linear increase in k_{obs} with increasing [DMA] was observed in the 0.2–0.8 M concentration range (Figure 1b, gray circles) and above this
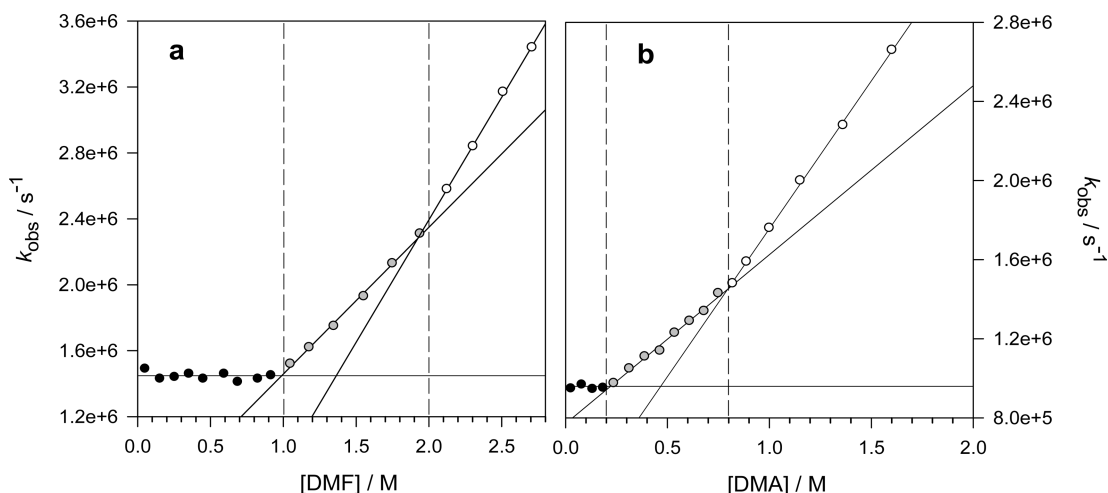

Figure 1. (a) Plot of the observed rate constant (k_{obs}) against [DMF] for reaction of the cumyloxyl radical (CumO[•]) measured at T = 25 °C in an argon-saturated acetonitrile solution containing 1.0 M dicumyl peroxide and 0.5 M LiClO$_4$, following 355 nm LFP. From the linear regression analysis in the 1.0–2.0 M [DMF] range (gray circles), k_{H1} = 8.91 × 10^5 M^{-1} s^{-1}, r^2 = 0.9972; in the 2.0–2.7 M [DMF] range (white circles), k_{H2} = 1.49 × 10^6 M^{-1} s^{-1}, r^2 = 0.9990. The dashed lines highlight [DMF] of 1.0 and 2.0 M. (b) Plot of the observed rate constant (k_{obs}) against [DMA] for reaction of the cumyloxyl radical (CumO[•]) measured at T = 25 °C in an argon-saturated acetonitrile solution containing 1.0 M dicumyl peroxide and 0.2 M LiClO$_4$, following 355 nm LFP. From the linear regression analysis in the 0.2–0.8 M [DMA] range (gray circles), k_{H1} = 8.54 × 10^5 M^{-1} s^{-1}, r^2 = 0.9918; in the 0.8–1.6 M [DMA] range (white circles), k_{H2} = 1.49 × 10^6 M^{-1} s^{-1}, r^2 = 0.9993. The dashed lines highlight [DMA] of 0.2 and 0.8 M.

concentration and with a different slope up to [DMA] = 1.6 M (Figure 1b, white circles). The HAT rate constants were obtained from the slope of the plots in the 0.2−0.8 and 0.8−1.6 M ranges as $k_{H1} = 8.54 \times 10^5$ M^{-1} s^{-1} and $k_{H2} = 1.49 \times 10^6$ M^{-1} s^{-1}, respectively.

It is well-established that Li$^+$ can strongly interact with the oxygen atom of DMF and DMA and that such interaction leads to an increase in C(O)−N bond order, to a corresponding decrease in C=O bond order, and to an overall increase in the extent of positive charge at nitrogen (Scheme 3, R = H, CH$_3$).[40]

Scheme 3
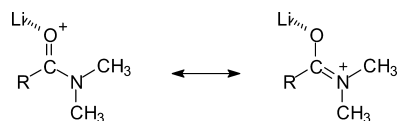
As pointed out previously, similar structural effects are also determined by the interaction of HBD solvents with the oxygen atom of amides.[36] Accordingly, in the study of kinetic solvent effects on HAT from DMF and DMA to CumO$^\bullet$, the greater than 2 orders of magnitude decrease in k_H measured on going from acetonitrile to the very strong HBD solvent 2,2,2-trifluoroethanol (TFE) was explained in terms of polar effects, where the increase in the electron deficiency of the C−H bonds of these substrates via solvent hydrogen bonding (Scheme 2) deactivates these bonds toward HAT to the electrophilic radical CumO$^\bullet$.[36]

On the basis of this picture, an analogous C−H deactivation will result from metal ion binding to the oxygen atom of DMF and DMA. Most importantly, however, previous studies have also shown that the lithium cation can efficiently bind more than one equivalent of amide[40] and, in particular, that DMF molecules bind to Li$^+$ with different strengths.[40b] Along these lines, the behavior observed in the reaction of CumO$^\bullet$ with DMF in acetonitrile containing 0.5 M LiClO$_4$ (Figure 1a) can be explained on the basis of the initial formation of a strongly bound 2:1 DMF−Li$^+$ complex, where interaction of the amide oxygen atom with the metal ion strongly deactivates the C−H bonds of DMF toward HAT. By considering that in acetonitrile, in the absence of added salt, HAT from DMF to CumO$^\bullet$ occurs with k_H(MeCN) = 1.32 × 10^6 M^{-1} s^{-1},[36] the negligible effect on k_{obs} observed up to 1.0 M DMF (Figure 1a, black circles) indicates that under these conditions only an upper limit to the rate constant for HAT from DMF can be determined as k_H < 1 × 10^4 M^{-1} s^{-1}, showing that the addition of LiClO$_4$ leads to a greater than 2 orders of magnitude decrease in HAT reactivity (k_H(MeCN)/k_H(Li$^+$) > 130) up to [DMF]/[Li$^+$] ≤ 2.[41] By increasing the concentration of DMF up to 2.0 M (Figure 1a, gray circles: 2 < [DMF]/[Li$^+$] ≤ 4), C−H deactivation is still observed, although to a relatively limited extent (k_H(MeCN)/k_{H1}(Li$^+$) = 1.5). This behavior clearly indicates that, as compared to the first two DMF molecules, binding of a third and fourth molecule to the lithium cation is significantly weaker, in full agreement with the previously proposed differential binding of DMF molecules to Li$^+$, explained in terms of increased steric crowding around the metal ion.[40b] For [DMF] > 2.0 M (Figure 1a, white circles, [DMF]/[Li$^+$] > 4), the k_{H2} value is very similar to the value measured in the absence of added salt (k_H(MeCN)/k_{H2}(Li$^+$) = 0.9), indicating that under these conditions the increase in k_{obs} reflects HAT from the C−H bonds of the free amide.

A very similar behavior was observed in the reaction of CumO$^\bullet$ with DMA (Figure 1b), where, however, differently than from DMF, strong C−H deactivation is now limited to one equivalent of amide, indicative of the formation of a strongly bound 1:1 DMA−Li$^+$ complex (Figure 1b, black circles). Above this concentration, a limited extent of C−H deactivation is observed (k_H(MeCN)/k_{H1}(Li$^+$) = 1.3, where k_H(MeCN) = 1.24 × 10^6 M^{-1} s^{-1};[32] see Table 1) up to 0.8 M DMA (Figure 1b, gray circles: 1 < [DMA]/[Li$^+$] ≤ 4). For [DMA] > 0.8 M (Figure 1b, white circles, [DMA]/[Li$^+$] > 4), the k_{H2} value is very similar to the value measured in the absence of added salt (k_H(MeCN)/k_{H2}(Li$^+$) = 0.8), indicating that also with this substrate the increase in k_{obs} now reflects HAT from the C−H bonds of the free amide.

When the reaction of CumO$^\bullet$ with DMF was studied in acetonitrile containing 0.5 M LiOTf (Figure 2), no significant
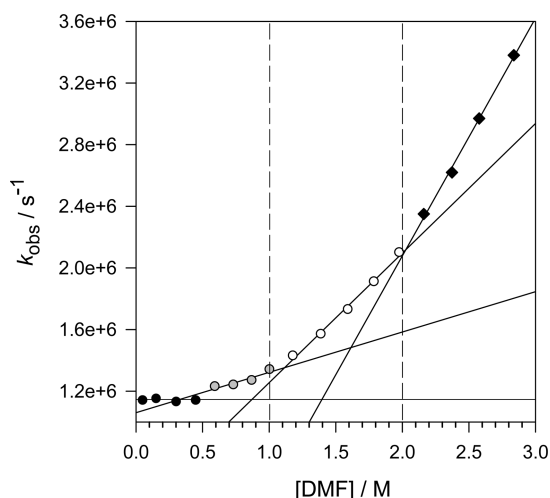
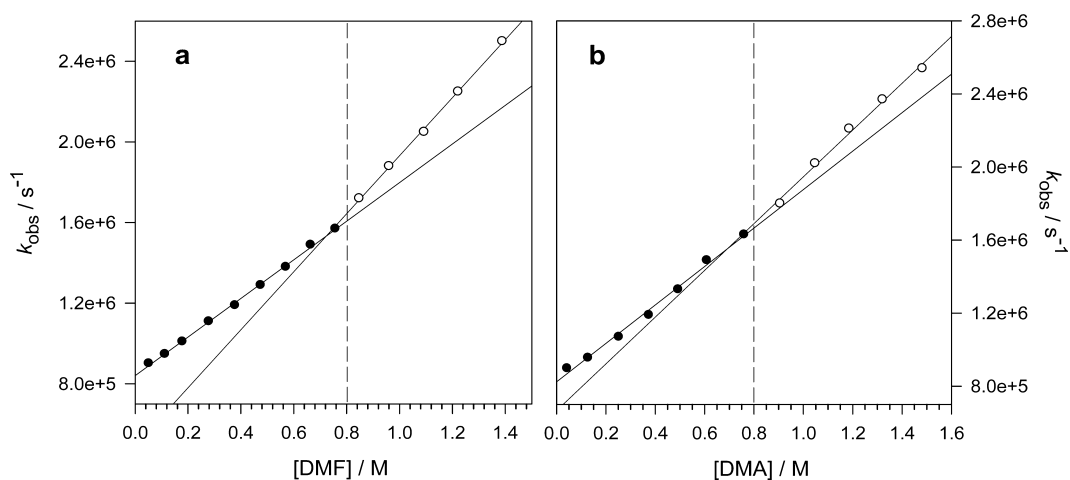**Figure 2.** Plot of the observed rate constant (k_{obs}) against [DMF] for reaction of the cumyloxyl radical (CumO$^\bullet$) measured at T = 25 °C in an argon-saturated acetonitrile solution containing 1.0 M dicumyl peroxide and 0.5 M LiOTf, following 355 nm LFP. From the linear regression analysis in the 0.5−1.0 M [DMF] range (gray circles), k_{H1} = 2.62 × 10^5 M^{-1} s^{-1}, r^2 = 0.89; in the 1.0−2.0 M [DMF] range (white circles), k_{H2} = 8.41 × 10^5 M^{-1} s^{-1}, r^2 = 0.9934; in the 2.0−2.7 M [DMF] range (black diamonds), k_{H3} = 1.54 × 10^6 M^{-1} s^{-1}, r^2 = 0.9970. The dashed lines highlight [DMF] of 1.0 and 2.0 M.

increase in k_{obs} was observed up to [DMF] = 0.5 M (black circles) and a linear increase in k_{obs} with increasing [DMF] was observed in the 0.5−1.0 M concentration range (gray circles) and, with progressively increasing slopes, in the 1.0−2.0 M (white circles) and 2.0−2.8 M (black diamonds) ranges.

The HAT rate constants were obtained from the slope of the plots in these three concentration ranges as k_{H1} = 2.62 × 10^5 M^{-1} s^{-1}, k_{H2} = 8.41 × 10^5 M^{-1} s^{-1}, and k_{H3} = 1.54 × 10^6 M^{-1} s^{-1}, respectively.

Comparison between LiClO$_4$ and LiOTf shows a behavior that is essentially identical for the two salts for [DMF] < 0.5 M and [DMF] > 1.0 M. The different behavior observed in the 0.5−1.0 M concentration range points toward a role for the lithium counteranion. The greater basicity in acetonitrile solution of TfO$^-$ as compared to that of ClO$_4^-$ (pK_a(MeCN) = 1.57 and 2.60 for HClO$_4$ and CF$_3$SO$_3$H, respectively)[42] suggests that Li$^+$ will be more strongly associated with the former anion as compared to the latter and will thus compete less efficiently for binding with a second DMF molecule,

Figure 3. (a) Plot of the observed rate constant (k_{obs}) against [DMF] for reaction of the cumyloxyl radical (CumO$^\bullet$) measured at $T = 25$ °C in an argon-saturated acetonitrile solution containing 1.0 M dicumyl peroxide and 0.2 M NaClO$_4$, following 355 nm LFP. From the linear regression analysis in the 0−0.8 M [DMF] range (black circles), $k_{H1} = 9.58 \times 10^5$ M^{-1} s^{-1}, $r^2 = 0.9987$; in the 0.8−1.4 M [DMF] range (white circles), $k_{H2} = 1.44 \times 10^6$ M^{-1} s^{-1}, $r^2 = 0.9990$. The dashed line highlights [DMF] of 0.8 M. (b) Plot of the observed rate constant (k_{obs}) against [DMA] for reaction of the cumyloxyl radical (CumO$^\bullet$) measured at $T = 25$ °C in an argon-saturated acetonitrile solution containing 1.0 M dicumyl peroxide and 0.2 M NaClO$_4$, following 355 nm LFP. From the linear regression analysis in the 0−0.8 M [DMA] range (black circles), $k_{H1} = 1.05 \times 10^6$ M^{-1} s^{-1}, $r^2 = 0.9938$; in the 0.8−1.5 M [DMA] range (white circles), $k_{H2} = 1.28 \times 10^6$ M^{-1} s^{-1}, $r^2 = 0.9933$. The dashed line highlights [DMA] of 0.8 M.
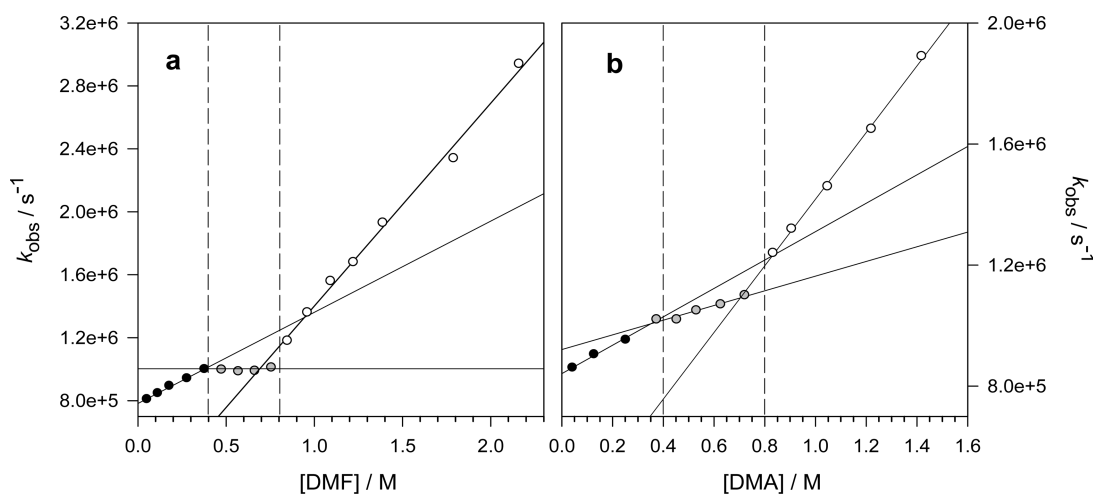
Figure 4. (a) Plot of the observed rate constant (k_{obs}) against [DMF] for reaction of the cumyloxyl radical (CumO$^\bullet$) measured at $T = 25$ °C in an argon-saturated acetonitrile solution containing 1.0 M dicumyl peroxide and 0.2 M Mg(ClO$_4$)$_2$, following 355 nm LFP. From the linear regression analysis in the 0−0.4 M [DMF] range (black circles), $k_{H1} = 5.79 \times 10^5$ M^{-1} s^{-1}, $r^2 = 0.9965$; in the 0.8−2.2 M [DMF] range (white circles), $k_{H2} = 1.29 \times 10^6$ M^{-1} s^{-1}, $r^2 = 0.9950$. The dashed lines highlight [DMF] of 0.4 and 0.8 M. (b) Plot of the observed rate constant (k_{obs}) against [DMA] for reaction of the cumyloxyl radical (CumO$^\bullet$) measured at $T = 25$ °C in an argon-saturated acetonitrile solution containing 1.0 M dicumyl peroxide and 0.2 M Mg(ClO$_4$)$_2$, following 355 nm LFP. From the linear regression analysis in the 0−0.4 M [DMA] range (black circles), $k_{H1} = 4.69 \times 10^5$ M^{-1} s^{-1}, $r^2 = 0.9951$; in the 0.4−0.8 M [DMA] range (gray circles), $k_{H2} = 2.43 \times 10^5$ M^{-1} s^{-1}, $r^2 = 0.96$; in the 0.8−1.4 M [DMA] range (white circles), $k_{H3} = 1.11 \times 10^6$ M^{-1} s^{-1}, $r^2 = 0.9988$. The dashed lines highlight [DMA] of 0.4 and 0.8 M.

leading to a smaller extent of C−H deactivation in the 0.5−1.0 M [DMF] range (compare Figures 1a and 2 in this concentration range).

Figure 3a,b shows the plots of k_{obs} vs [substrate] for the reactions of DMF and DMA with CumO$^\bullet$ in acetonitrile containing 0.2 M NaClO$_4$.

With both DMF and DMA, a linear increase in k_{obs} with increasing substrate concentration was observed up to 0.8 M (black circles) and above this concentration and with a different slope up to 1.5 M (white circles). The HAT rate constants were obtained from the slope of the plots in the two concentration ranges as $k_{H1} = 9.58 \times 10^5$ M^{-1} s^{-1} and $k_{H2} = 1.44 \times 10^6$ M^{-1} s^{-1} and $k_{H1} = 1.05 \times 10^6$ M^{-1} s^{-1} and $k_{H2} = 1.28 \times 10^6$ M^{-1} s^{-1},

for DMF and DMA, respectively. These results clearly show that in the reaction of CumO$^\bullet$ with DMF and DMA the addition of NaClO$_4$ leads to a very limited extent of C−H deactivation up to [substrate] ≤ 0.8 M (k_H(MeCN)/k_{H1}(Na$^+$) = 1.2−1.4), indicative of a relatively weak binding of the sodium cation to the amide up to [substrate]/[Na$^+$] ≤ 4. The linear dependence observed in this concentration range suggests, moreover, that Na$^+$ can bind, with comparable strength, four substrate molecules. For [substrate] > 0.8 M, the measured k_{H2} values are very similar to the values measured in the absence of added salt (k_H(MeCN)/k_{H2}(Na$^+$) = 0.9−1.0), indicating that under these conditions the increase in k_{obs} reflects HAT from the C−H bonds of the free amides. As

E

compared to the experiments carried out in the presence of LiClO$_4$, where strong C−H deactivation was observed for the first two DMF equivalents and the first DMA equivalent followed by a significantly weaker deactivation up to the fourth substrate equivalent, the different behavior observed with NaClO$_4$ can be conveniently explained on the basis of the stronger Lewis acidity of Li$^+$ as compared to that of Na$^{+[43]}$ and of the greater size of the latter cation,[44] for which steric crowding following substrate binding is expected to be relatively less important.

Figure 4a,b shows the plots of k_{obs} vs [substrate] for the reactions of DMF and DMA with CumO$^\bullet$ in acetonitrile containing 0.2 M Mg(ClO$_4$)$_2$. In the reaction with DMF, a linear increase in k_{obs} with increasing [DMF] was observed up to 0.4 M (Figure 4a, black circles). Above this concentration, no significant increase in k_{obs} was observed between 0.4 and 0.8 M (Figure 4a, gray circles), and a linear increase in k_{obs} with increasing [DMF] was observed in the 0.8−2.2 M concentration range (Figure 4a, white circles).

The HAT rate constants were obtained from the slope of the plots in the 0−0.4 and 0.8−2.2 M concentration ranges as k_{H1} = 5.79 × 10^5 M^{-1} s^{-1} and k_{H2} = 1.29 × 10^6 M^{-1} s^{-1}, respectively. An analogous behavior was observed when the reaction of CumO$^\bullet$ with DMF was carried out in the presence of 0.5 and 1.0 M Mg(ClO$_4$)$_2$ and when employing 266 nm LFP for CumO$^\bullet$ generation (Figure S4).

In the reaction with DMA, linear increases in k_{obs} with increasing [DMA] were observed, with different slopes, in the 0−0.4 M (Figure 4b, black circles), 0.4−0.8 M (Figure 4b, gray circles), and 0.8−1.4 M (Figure 4b, white circles) concentration ranges. The HAT rate constants were obtained from the slope of the plots in the three concentration ranges as k_{H1} = 4.69 × 10^5 M^{-1} s^{-1}, k_{H2} = 2.43 × 10^5 M^{-1} s^{-1}, and k_{H3} = 1.11 × 10^6 M^{-1} s^{-1}, respectively.

These behaviors can be explained on the basis of the initial formation of relatively weakly bound 2:1 amide−Mg^{2+} complexes, where interaction of the metal ion with the amide oxygen atom deactivates, to a limited extent, the C−H bonds of DMF and DMA toward HAT to CumO$^\bullet$ (k_H(MeCN)/k_{H1}(Mg^{2+}) = 2.3−2.6). The negligible effect on k_{obs} observed in the 0.4−0.8 M [DMF] range (Figure 4a, gray circles: 2 < [DMF]/[Mg^{2+}] ≤ 4) is indicative of strong C−H deactivation, where, as compared to the first two DMF molecules, significantly stronger binding of a third and fourth molecule to the magnesium cation occurs. As compared to DMF, a lower extent of deactivation is instead observed for DMA in the same concentration range (k_H(MeCN)/k_{H2}(Mg^{2+}) = 5.1), deactivation that is nevertheless more pronounced than that observed in the 0−0.4 M [DMA] range. This different behavior indicates that in this concentration range interaction with Mg^{2+} is weaker for DMA than for DMF. The hypothesis of a weaker binding of DMA to the metal cations is also supported by the evidence provided above for the formation of strongly bound 2:1 DMF−Li$^+$ and 1:1 DMA−Li$^+$ complexes (Figure 1a,b) and by the observation of a slightly lower extent of C−H bond deactivation for DMA as compared to that for DMF in the presence of Na$^+$ (Figure 3,b). As DMA is characterized by a slightly higher Lewis basicity than DMF (DN = 26.6 and 27.8 kcal mol^{-1}, for DMF and DMA, respectively),[30] the stronger interaction of DMF with the metal cations points toward a role for steric effects associated with the increase in steric hindrance determined by replacement of the formyl hydrogen in DMF with a methyl group in DMA. This hypothesis suggests,

moreover, that binding of the metal cations to the amide oxygen atom occurs from the opposite side of the C−N bond, as shown in Scheme 3.
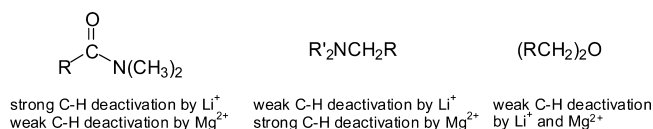
For [amide] > 0.8 M ([amide]/[Mg^{2+}] > 4), the k_{H2} and k_{H3} values (for DMF and DMA, respectively) are very similar to the values measured in the absence of added salt (k_H(MeCN)/k_{H2}(Mg^{2+}) = 1.0 and k_H(MeCN)/k_{H3}(Mg^{2+}) = 0.9 for DMF and DMA, respectively), indicating that under these conditions the increase in k_{obs} reflects HAT from the C−H bonds of the free amides.

Comparison between the plots displayed in Figures 1a,b and 4a,b shows that the interaction of DMF and DMA with LiClO$_4$ and Mg(ClO$_4$)$_2$ leads to significantly different kinetic effects on HAT from the C−H bonds of these substrates to CumO$^\bullet$. As mentioned above, with LiClO$_4$, the kinetic data point toward the formation of strongly bound 2:1 DMF−Li$^+$ and 1:1 DMA−Li$^+$ complexes, resulting in strong C−H bond deactivation, followed by a weaker interaction with two and three additional DMF and DMA molecules that leads to a limited extent of C−H bond deactivation. With Mg(ClO$_4$)$_2$, formation of weakly bound 2:1 amide−Mg^{2+} complexes, resulting in limited C−H bond deactivation, is observed with both substrates, followed by a stronger interaction with two additional molecules, which now determines, as compared to the first concentration range, a very strong deactivation of the C−H bonds of DMF and a relatively stronger deactivation of the C−H bonds of DMA.

Although at present we do not have a clear-cut explanation for the peculiar kinetic behavior observed in the presence of Mg(ClO$_4$)$_2$, the greater charge density of Mg^{2+} than of Li$^+$ as well as the different coordination geometries of the two ions, a rigid octahedral ligation sphere with Mg^{2+} resulting from a stable coordination number (almost invariably 6), as compared to the most common coordination number of 4 for Li$^+$, can be reasonably expected to account for this different behavior.[4,11,44−46] Both factors suggest that interaction with the perchlorate counteranion will be relatively more important for Mg^{2+} than for Li$^+$, possibly influencing binding of the amide substrates to the metal cations and, as a consequence, the C−H bond deactivation patterns. In addition, it is well-established that Mg^{2+} interacts significantly more strongly than Li$^+$ with acetonitrile[47] and that both cations interact more strongly with amide substrates than with acetonitrile.[48] Accordingly, the differential solvation experienced by Mg^{2+} and Li$^+$ in acetonitrile after addition of the amides may also be responsible for the different behavior observed in the presence of these two metal cations.[46] Despite of these reasonable, although tentative, explanations, it appears that, in order to provide a better understanding of the effect of Mg^{2+} on HAT from the C−H bonds of alkanamides, additional studies are certainly needed.

Most importantly, as compared to the reactions of DMF and DMA, an opposite behavior was observed for the reactions of CumO$^\bullet$ with tertiary aliphatic amines in acetonitrile after addition of LiClO$_4$ and Mg(ClO$_4$)$_2$. In HAT from triethylamine, triisobutylamine, and 1,2,2,6,6-pentamethylpiperidine, a 2-fold decrease in k_H was measured after addition of LiClO$_4$, whereas a greater than 2 orders of magnitude decrease in k_H was measured after addition of Mg(ClO$_4$)$_2$.[25] Comparison between the results obtained with these two classes of substrates suggests that the addition of up to two equivalents of lithium and magnesium salts, as compared to the substrate, can be used in an orthogonal fashion to control the selectivity in HAT-based C−H functionalization of substrates bearing both amide and amine functionalities. While Li$^+$ is expected to

strongly deactivate the C–H bonds in proximity of an amide group and only to a limited extent the C–H bonds that are α to an amine nitrogen atom, an opposite effect is expected with Mg^{2+} (Figure 5).

R–C(=O)–N(CH₃)₂

strong C–H deactivation by Li⁺
weak C–H deactivation by Mg²⁺

R'₂NCH₂R

weak C–H deactivation by Li⁺
strong C–H deactivation by Mg²⁺

(RCH₂)₂O

weak C–H deactivation by Li⁺ and Mg²⁺

Figure 5. Qualitative representation of the extent of deactivation of the C–H bonds of aliphatic amides, amines, and ethers toward HAT to CumO$^\bullet$, determined by interaction with Li$^+$ and Mg^{2+}.

In other words, selective protection of the proximal C–H bonds of amine or amide functionalities toward HAT to electrophilic radicals can be achieved by proper selection of the metal ion salt. Along these lines, the 2- to 3-fold decrease in k_H measured in acetonitrile after addition of LiClO$_4$ or Mg-(ClO$_4$)$_2$, for HAT from the α-C–H bonds of THF to CumO$^\bullet$,[25] indicates that these salts can be also employed for the selective deactivation of amide (LiClO$_4$) and amine (Mg(ClO$_4$)$_2$) functionalities in the presence of ether functionalities. The possibility of achieving site-selective C–H deactivation via metal ion binding appears to be of great interest in view of the large number of synthetically useful C–H functionalization procedures based on HAT from amides, amines, and ethers to alkoxyl and other electrophilic hydrogen atom abstracting species.[31,49]

Figure 6a,b shows the plots of k_{obs} vs [substrate] for the reactions of DMF and DMA with CumO$^\bullet$ in acetonitrile containing 0.2 M Ca(ClO$_4$)$_2$.

With both DMF and DMA, a decrease in k_{obs} with increasing substrate concentration was observed up to 0.2 M (black circles), no significant increase in k_{obs} was observed between 0.2 and 0.7–0.8 M (gray circles), and a linear increase in k_{obs} with increasing amide concentration was then observed between 0.7–1.6 and 0.8–1.8 M (white circles). The HAT rate

constants were obtained from the slope of the plots in the latter concentration range as $k_{H1} = 1.04 \times 10^6$ M^{-1} s^{-1} and $k_{H1} = 1.24 \times 10^6$ M^{-1} s^{-1} for DMF and DMA, respectively. The decrease in k_{obs} observed in the 0–0.2 M [amide] range can be reasonably explained on the basis of the effect of the metal cation on the rate constant for CumO$^\bullet$ C–CH$_3$ β-scission (k_β, eq 1) and of the competition between CumO$^\bullet$ and the amide substrate for Ca^{2+}. Previous studies have clearly shown that in acetonitrile solution the addition of metal ion salts (LiClO$_4$, NaClO$_4$, and Mg(ClO$_4$)$_2$) leads to an increase in the CumO$^\bullet$ k_β.[25] This behavior was explained on the basis of the interaction of the metal cation (M^{n+}) with the oxygen atom of CumO$^\bullet$. This interaction increases in strength on going from CumO$^\bullet$ to the β-scission transition state, characterized by an incipient carbonyl group character (Scheme 4), leading to a stabilization of the transition state and to a corresponding increase in k_β as compared to acetonitrile.

Scheme 4
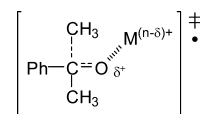
Along this line, the effect of LiClO$_4$, NaClO$_4$, Mg(ClO$_4$)$_2$, and Ca(ClO$_4$)$_2$ on k_β was investigated at $T = 25$ °C following 355 nm LFP of argon-saturated acetonitrile solutions containing 1.0 M dicumyl peroxide and 0.2 M metal ion salt. The following rate constants were measured: $k_\beta = 1.34 \times 10^6$, 1.01×10^6, 8.96×10^5, and 8.41×10^5 s^{-1} for Ca^{2+}, Li$^+$, Mg^{2+}, and Na$^+$, respectively (as compared to $k_\beta = 7.60 \times 10^5$ s^{-1}, measured under the same experimental conditions in the absence of added salt), showing that among these metal cations Ca^{2+} exhibits the strongest kinetic effect on CumO$^\bullet$ β-scission. These results indicate that by addition of the relatively strong Lewis basic amides DMF and DMA to acetonitrile solutions containing 0.2 M Ca(ClO$_4$)$_2$ efficient competition with CumO$^\bullet$
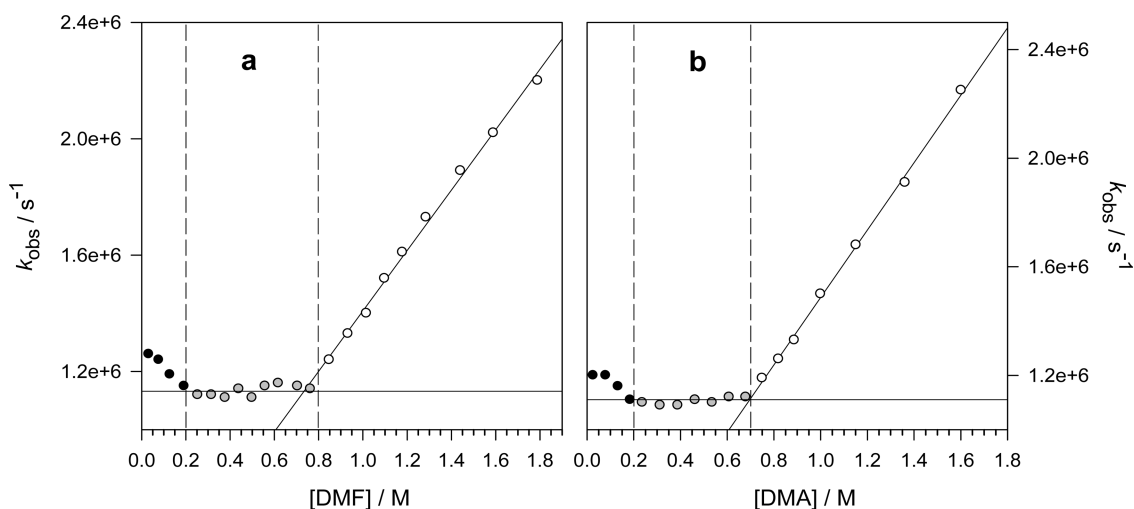
Figure 6. (a) Plot of the observed rate constant (k_{obs}) against [DMF] for reaction of the cumyloxyl radical (CumO$^\bullet$) measured at $T = 25$ °C in an argon-saturated acetonitrile solution containing 1.0 M dicumyl peroxide and 0.2 M Ca(ClO$_4$)$_2$, following 355 nm LFP. From the linear regression analysis in the 0.8–1.8 M [DMF] range (white circles), $k_{H1} = 1.04 \times 10^6$ M^{-1} s^{-1}, $r^2 = 0.9963$. The dashed lines highlight [DMF] of 0.2 and 0.8 M. (b) Plot of the observed rate constant (k_{obs}) against [DMA] for reaction of the cumyloxyl radical (CumO$^\bullet$) measured at $T = 25$ °C in an argon-saturated acetonitrile solution containing 1.0 M dicumyl peroxide and 0.2 M Ca(ClO$_4$)$_2$, following 355 nm LFP. From the linear regression analysis in the 0.7–1.6 M [DMA] range (white circles), $k_{H1} = 1.24 \times 10^6$ M^{-1} s^{-1}, $r^2 = 0.9982$. The dashed lines highlight [DMA] of 0.2 and 0.7 M.

Table 2. Second-Order Rate Constants (k_H) for the Reaction of the Cumyloxyl Radical (CumO$^\bullet$) with *N,N*-Dimethylformamide (DMF) and *N,N*-Dimethylacetamide (DMA) Measured in DMSO in the Presence of Metal Ion Salts

	k_H/M^{-1} s^{-1a}		
	DMSO	0.2 M LiClO$_4$	0.2 M Mg(ClO$_4$)$_2$
DMF	$2.50 \pm 0.06 \times 10^{6b}$	$2.55 \pm 0.02 \times 10^6$	$2.78 \pm 0.02 \times 10^6$
DMA	$2.41 \pm 0.05 \times 10^{6b}$	$2.45 \pm 0.03 \times 10^6$	$3.04 \pm 0.06 \times 10^6$

[a]Measured in argon-saturated solution at $T = 25$ °C employing 355 nm LFP, [dicumyl peroxide] = 1.0 M, from the slope of the k_{obs} vs [substrate] plots, where, in turn, k_{obs} values were measured following the decay of the CumO$^\bullet$ visible absorption band at 490 nm. Average of at least two determinations. [b]Table 1.

for Ca^{2+} occurs, leading to a decrease in k_β, reflected into the measured k_{obs} values, up to [amide] = [Ca(ClO$_4$)$_2$], thus accounting for the behavior described above in the 0−0.2 M concentration range (Figure 6a,b, black circles). The observation of a slight decrease in k_{obs} after addition of DMF to an acetonitrile solution containing 0.5 M LiClO$_4$ in the initial region of the k_{obs} vs [DMF] plot (see Figure 1a) is also consistent with this hypothesis.

On the basis of this picture, the kinetic data displayed in Figure 6a,b indicate that in the reaction of CumO$^\bullet$ with DMF and DMA Ca^{2+} can strongly bind up to four substrate molecules, leading to strong C−H bond deactivation over this concentration range ([amide]/[Ca^{2+}] ≤ 4).

Interestingly, the kinetic data discussed above show that, among the four metal cations investigated, Na$^+$ and Ca^{2+} are able to bind up to four substrate molecules with comparable strength, whereas differential binding of up to four substrate molecules is observed with Li$^+$ and Mg^{2+}. These binding patterns clearly show that the size of the metal cation plays an important role as the former two cations are characterized by a significantly larger size as compared to the latter ones,[44] thus limiting the influence of steric crowding on the binding of multiple substrate molecules.

For [amide] > 0.7−0.8 M ([amide]/[Ca^{2+}] > 3.5−4), the k_{H1} values are very similar to the values measured in the absence of added salt (k_H(MeCN)/k_{H1}(Ca^{2+}) = 1.0−1.3), indicating that the increase in k_{obs} now reflects HAT from the C−H bonds of the free amides.

The effect of LiClO$_4$ and Mg(ClO$_4$)$_2$ on HAT from DMF and DMA to CumO$^\bullet$ was also studied in DMSO, a solvent characterized by a significantly higher Lewis basicity than acetonitrile (DN = 29.8 and 14.1 kcal mol^{-1} for DMSO and MeCN, respectively).[30] The k_{obs} vs [substrate] plots for the reactions of CumO$^\bullet$ with DMF and DMA in DMSO solutions containing 0.2 M LiClO$_4$ or Mg(ClO$_4$)$_2$, at $T = 25$ °C, are displayed in the Supporting Information (Figures S5−S8). The k_H values thus obtained are collected in Table 2. As a matter of comparison, also included in this table are the corresponding k_H values measured in DMSO in the absence of metal ion salt.

The data collected in Table 2 show that no significant difference in k_H is observed after addition of 0.2 M LiClO$_4$, whereas a slight increase in k_H is observed in the presence of 0.2 M Mg(ClO$_4$)$_2$ ((k_H(DMSO)/k_{H1}(Mg^{2+})) = 0.9 and 0.8 for DMF and DMA, respectively). As compared to acetonitrile, where, as mentioned above, strong deactivation was observed after addition of these metal ion salts, no C−H deactivation occurs in DMSO, clearly indicating that this solvent out-competes DMF and DMA for Li$^+$ and Mg^{2+} binding, in line with its strong Lewis basicity and its high concentration. On the basis of this observation, under these conditions specific interactions between the metal cations and the amides can be excluded and, accordingly, the slight increase in k_H observed

after addition of Mg(ClO$_4$)$_2$ can be reasonably explained on the basis of salt effects in line with the increase in polarity on going from the reactants to the transition state for HAT from these substrates to CumO$^\bullet$ discussed above (see, for example, Schemes 1 and 2).

■ CONCLUSIONS

Taken together, the results presented above clearly show that the addition of redox-inactive alkali and alkaline earth metal ion salts can strongly influence the HAT reactivity of tertiary amides toward alkoxyl radicals. Metal ion binding to the oxygen atom of DMF and DMA determines an increase in the extent of positive charge on the amide nitrogen and of the electron deficiency of the C−H bonds of these substrates, leading to their deactivation toward HAT to an electrophilic radical such as CumO$^\bullet$. In acetonitrile, strong deactivating effects are observed in the presence of Li$^+$ and Ca^{2+}, which can efficiently bind up to two and four equivalents of the amide substrate. A mixed behavior is observed with Mg^{2+}, characterized by a relatively weak deactivation for the first two substrate equivalents followed by a stronger deactivation for two additional equivalents. Very limited C−H deactivation is instead observed in the presence of Na$^+$. No C−H deactivation was observed in DMSO after addition of Li$^+$ and Mg^{2+}, in line with the significantly weaker Lewis basicity of acetonitrile as compared to that of DMSO. These different reactivity patterns reflect the influence of Lewis acidity and size of the metal cation and of solvent Lewis basicity on the interaction with the amide substrate. Most importantly, the results obtained in this study clearly indicate that by varying the nature of the metal cation, the counteranion, and the solvent, C−H deactivation can be modulated, allowing careful control over the HAT reactivity of amide substrates toward electrophilic radicals. The detailed knowledge of the effect of metal ion salts on HAT from amides, coupled with the results of previous studies on the effect of lithium and magnesium salts on HAT from aliphatic amines and ethers, indicates moreover that, through proper selection of the metal ion salt, control over selectivity in the HAT-based C−H functionalization of substrates bearing different functionalities can be achieved. This aspect appears to be of great interest in view of the increasing number of synthetically useful C−H functionalization procedures based on HAT to alkoxyl and other electrophilic hydrogen atom abstracting species.

As a final consideration, amides are often employed as simple models for the peptide bond. Along this line, on the basis of the strong deactivation of the C−H bonds of DMF and DMA toward HAT to CumO$^\bullet$ observed after addition of alkali and alkaline earth metal ion salts, similar effects may also be expected in the corresponding reactions of peptides and proteins, suggesting that binding to these metal ions can protect the C−H bonds of these molecules from HAT to

reactive oxygen centered radicals. Further studies, under way in our laboratory, will probe this intriguing issue.

EXPERIMENTAL SECTION

Materials. Spectroscopic grade acetonitrile and DMSO were used in the kinetic experiments. Dicumyl peroxide was of the highest commercial quality available and was used as received. N,N-Dimethylformamide (DMF) and N,N-dimethylacetamide (DMA) were of the highest commercial quality available and were used as received.

Lithium perchlorate ($LiClO_4$), lithium trifluoromethanesulfonate (LiOTf), sodium perchlorate ($NaClO_4$), magnesium perchlorate ($Mg(ClO_4)_2$), and calcium perchlorate ($Ca(ClO_4)_2$) were of the highest commercial quality available and were used as received without any drying procedure.

Laser Flash Photolysis Studies. LFP experiments were carried out with a laser kinetic spectrometer using the third (355 nm) or fourth harmonic (266 nm) of a Q-switched Nd:YAG laser, delivering 8 ns pulses. The laser energy was adjusted to ≤10 mJ/pulse by the use of the appropriate filter. A 3.5 mL Suprasil quartz cell (10 mm × 10 mm) was used in all experiments. Argon saturated acetonitrile or DMSO solutions containing dicumyl peroxide (10 mM for 266 nm LFP and 1.0 M for 355 nm LFP) were employed. All experiments were carried out at $T = 25 \pm 0.5$ °C under magnetic stirring. The observed rate constants (k_{obs}) were obtained by averaging 2−5 individual values and were reproducible to within 5%.

Second-order rate constants for the reactions of the cumyloxyl radical with DMF and DMA in the presence of metal ion salts were obtained from the slopes of the k_{obs} (measured following the decay of the cumyloxyl radical visible absorption band at 490 nm) vs [substrate] plots at constant salt concentration (between 0.2 and 1.0 M). Fresh solutions were used for every substrate concentration. The concentration variation was performed through direct addition of the substrate to solutions containing dicumylperoxide and the metal ion salt. Where available, the given rate constants are the average of at least two independent experiments, with typical errors being ≤10%.

ASSOCIATED CONTENT

⑤ Supporting Information

The Supporting Information is available free of charge on the ACS Publications website at DOI: 10.1021/acs.joc.5b01661.

Plots of k_{obs} vs substrate concentration for the reactions of CumO$^\bullet$ (PDF).

AUTHOR INFORMATION

Corresponding Author
*E-mail: bietti@uniroma2.it.

Notes
The authors declare no competing financial interest.

ACKNOWLEDGMENTS

REFERENCES

(1) (a) Savelyev, A.; MacKerell, A. D., Jr. *J. Phys. Chem. B* **2015**, *119*, 4428−4440. (b) Savelyev, A.; MacKerell, A. D., Jr. *J. Phys. Chem. Lett.* **2015**, *6*, 212−216.

(2) Owczarzy, R.; Moreira, B. G.; You, Y.; Behlke, M. A.; Walder, J. A. *Biochemistry* **2008**, *47*, 5336−5353.

(3) Hud, N. V.; Polak, M. *Curr. Opin. Struct. Biol.* **2001**, *11*, 293−301.

(4) (a) Dudev, T.; Lim, C. *Chem. Rev.* **2014**, *114*, 538−556. (b) Dudev, T.; Lim, C. *Acc. Chem. Res.* **2014**, *47*, 3580−3587.

(5) Johnson, R. P.; Fleming, A. M.; Burrows, C. J.; White, H. S. *J. Phys. Chem. Lett.* **2014**, *5*, 3781−3786.

(6) Shi, J.; Wang, J. *J. Phys. Chem. B* **2014**, *118*, 12336−12347.

(7) Kundu, P. P.; Bhowmick, T.; Swapna, G.; Pavan Kumar, G. V.; Nagaraja, V.; Narayana, C. *J. Phys. Chem. B* **2014**, *118*, 5322−5330.

(8) Wang, Z.; Sapienza, P. J.; Abeysinghe, T.; Luzum, C.; Lee, A. L.; Finer-Moore, J. S.; Stroud, R. M.; Kohen, A. *J. Am. Chem. Soc.* **2013**, *135*, 7583−7592.

(9) Rembert, K. B.; Paterová, J.; Heyda, J.; Hilty, C.; Jungwirth, P.; Cremer, P. S. *J. Am. Chem. Soc.* **2012**, *134*, 10039−10046.

(10) Valdez, C. E.; Smith, Q. A.; Nechay, M. R.; Alexandrova, A. N. *Acc. Chem. Res.* **2014**, *47*, 3110−3117.

(11) Babu, C. S.; Dudev, T.; Lim, C. *J. Am. Chem. Soc.* **2013**, *135*, 6541−6548.

(12) (a) Yano, J.; Yachandra, V. *Chem. Rev.* **2014**, *114*, 4175−4205. (b) Grundmeier, A.; Dau, H. *Biochim. Biophys. Acta, Bioenerg.* **2012**, *1817*, 88−105. (c) McEvoy, J. P.; Brudvig, G. W. *Chem. Rev.* **2006**, *106*, 4455−4483.

(13) (a) Yang, J.; Hatakeyama, M.; Ogata, K.; Nakamura, S.; Li, C. *J. Phys. Chem. B* **2014**, *118*, 14215−14222. (b) Chatterjee, R.; Milikisiyants, S.; Coates, C. S.; Koua, F. H. M.; Shen, J.-R.; Lakshmi, K. V. *Phys. Chem. Chem. Phys.* **2014**, *16*, 20834−20843.

(14) Lee, Y.-M.; Bang, S.; Kim, Y. M.; Cho, J.; Hong, S.; Nomura, T.; Ogura, T.; Troeppner, O.; Ivanović-Burmazović, I.; Sarangi, R.; Fukuzumi, S.; Nam, W. *Chem. Sci.* **2013**, *4*, 3917−3923.

(15) Li, F.; Van Heuvelen, K. M.; Meier, K. K.; Münck, E.; Que, L., Jr. *J. Am. Chem. Soc.* **2013**, *135*, 10198−10201.

(16) Bang, S.; Lee, Y.-M.; Hong, S.; Cho, K.-B.; Nishida, Y.; Seo, M. S.; Sarangi, R.; Fukuzumi, S.; Nam, W. *Nat. Chem.* **2014**, *6*, 934−940.

(17) (a) Waki, T.; Kobayashi, S.; Matsumoto, K.; Ozawa, T.; Kamada, T.; Nakanishi, I. *Chem. Commun.* **2013**, *49*, 9842−9844. (b) Nakanishi, I.; Kawashima, T.; Ohkubo, K.; Kanazawa, H.; Inami, K.; Mochizuki, M.; Fukuhara, K.; Okuda, H.; Ozawa, T.; Itoh, S.; Fukuzumi, S.; Ikota, N. *Org. Biomol. Chem.* **2005**, *3*, 626−629. (c) Nakanishi, I.; Miyazaki, K.; Shimada, T.; Ohkubo, K.; Urano, S.; Ikota, N.; Ozawa, T.; Fukuzumi, S.; Fukuhara, K. *J. Phys. Chem. A* **2002**, *106*, 11123−11126. (d) Nakanishi, I.; Fukuhara, K.; Shimada, T.; Ohkubo, K.; Iizuka, Y.; Inami, K.; Mochizuki, M.; Urano, S.; Itoh, S.; Miyata, N.; Fukuzumi, S. *J. Chem. Soc., Perkin Trans. 2* **2002**, 1520−1524.

(18) (a) Mukai, K.; Oi, M.; Ouchi, A.; Nagaoka, S. *J. Phys. Chem. B* **2012**, *116*, 2615−2621. (b) Kohno, Y.; Fujii, M.; Matsuoka, C.; Hashimoto, H.; Ouchi, A.; Nagaoka, S.; Mukai, K. *J. Phys. Chem. B* **2011**, *115*, 9880−9888. (c) Ouchi, A.; Nagaoka, S.; Abe, K.; Mukai, K. *J. Phys. Chem. B* **2009**, *113*, 13322−13331.

(19) (a) Nam, W.; Lee, Y.-M.; Fukuzumi, S. *Acc. Chem. Res.* **2014**, *47*, 1146−1154. (b) Hong, S.; Pfaff, F. F.; Kwon, E.; Wang, Y.; Seo, M.-S.; Bill, E.; Ray, K.; Nam, W. *Angew. Chem., Int. Ed.* **2014**, *53*, 10403−10407.

(20) Thazhathveetil, A. K.; Trifonov, A.; Wasielewski, M. R.; Lewis, F. D. *J. Phys. Chem. A* **2014**, *118*, 10359−10363.

(21) (a) Tsui, E. Y.; Tran, R.; Yano, J.; Agapie, T. *Nat. Chem.* **2013**, *5*, 293−299. (b) Risch, M.; Klingan, K.; Ringleb, F.; Chernev, P.; Zaharieva, I.; Fischer, A.; Dau, H. *ChemSusChem* **2012**, *5*, 542−549. (c) Wiechen, M.; Zaharieva, I.; Dau, H.; Kurz, P. *Chem. Sci.* **2012**, *3*, 2330−2339.

(22) Chen, J.; Lee, Y.-M.; Davis, K. M.; Wu, X.; Seo, M. S.; Cho, K.-B.; Yoon, H.; Park, Y. J.; Fukuzumi, S.; Pushkar, Y. N.; Nam, W. *J. Am. Chem. Soc.* **2013**, *135*, 6388−6391.

(23) Leeladee, P.; Baglia, R. A.; Prokop, K. A.; Latifi, R.; de Visser, S. P.; Goldberg, D. P. *J. Am. Chem. Soc.* **2012**, *134*, 10397−10400.

(24) Morimoto, Y.; Park, J.; Suenobu, T.; Lee, Y.-M.; Nam, W.; Fukuzumi, S. *Inorg. Chem.* **2012**, *51*, 10025−10036.

(25) Salamone, M.; Mangiacapra, L.; DiLabio, G. A.; Bietti, M. *J. Am. Chem. Soc.* **2013**, *135*, 415−423.

(26) Nova, A.; Balcells, D. *Chem. Commun.* **2014**, *50*, 614−616.

(27) Mitroka, S.; Zimmeck, S.; Troya, D.; Tanko, J. M. *J. Am. Chem. Soc.* **2010**, *132*, 2907−2913.

(28) Roberts, B. P. *Chem. Soc. Rev.* **1999**, *28*, 25−35.

(29) Lewis basicity can be expressed in terms of Gutmann's donor number (*DN*), defined as the negative ΔH value for 1:1 adduct formation between $SbCl_5$ and electron-pair donor solvents in the noncoordinating solvent 1,2-dichloroethane. For example, DN = 26.6 and 27.8 kcal mol^{-1} for *N,N*-dimethylformamide (DMF) and *N,N*-dimethylacetamide (DMA), respectively.[30]

(30) Reichardt, C.; Welton, T. *Solvents and Solvent Effects in Organic Chemistry*, 4th ed.; Wiley-VCH: Weinheim, Germany, 2010.

(31) See, for example: (a) Saidulu, G.; Kumar, R. A.; Reddy, K. R. *Tetrahedron Lett.* **2015**, *56*, 4200−4203. (b) Tu, H.-Y.; Liu, Y.-R.; Chu, J.-J.; Hu, B.-L.; Zhang, X.-G. *J. Org. Chem.* **2014**, *79*, 9907−9912. (c) Yang, X.-H.; Wei, W.-T.; Li, H.-B.; Song, R.-J.; Li, J.-H. *Chem. Commun.* **2014**, *50*, 12867−12869. (d) Yu, H.; Shen, J. *Org. Lett.* **2014**, *16*, 3204−3207. (e) Feng, J.-B.; Wei, D.; Gong, J.-L.; Qi, X.; Wu, X.-F. *Tetrahedron Lett.* **2014**, *55*, 5082−5084. (f) Wang, R.; Liu, H.; Yue, L.; Zhang, X.-K.; Tan, Q.-Y.; Pan, R.-L. *Tetrahedron Lett.* **2014**, *55*, 2233−2237. (g) Kumar, G. S.; Kumar, R. A.; Kumar, P. S.; Reddy, N. V.; Kumar, K. V.; Kantam, M. L.; Prabhakar, S.; Reddy, K. R. *Chem. Commun.* **2013**, *49*, 6686−6688. (h) Li, D.; Wang, M.; Liu, J.; Zhao, Q.; Wang, L. *Chem. Commun.* **2013**, *49*, 3640−3642. (i) Wang, H.; Guo, L.-N.; Duan, X.-H. *Org. Biomol. Chem.* **2013**, *11*, 4573−4576. (j) Ding, S.; Jiao, N. *Angew. Chem., Int. Ed.* **2012**, *51*, 9226−9237.

(32) Salamone, M.; Milan, M.; DiLabio, G. A.; Bietti, M. *J. Org. Chem.* **2013**, *78*, 5909−5917.

(33) Baciocchi, E.; Bietti, M.; Salamone, M.; Steenken, S. *J. Org. Chem.* **2002**, *67*, 2266−2270.

(34) Avila, D. V.; Ingold, K. U.; Di Nardo, A. A.; Zerbetto, F.; Zgierski, M. Z.; Lusztyk, J. *J. Am. Chem. Soc.* **1995**, *117*, 2711−2718.

(35) Salamone, M.; Bietti, M. *Synlett* **2014**, *25*, 1803−1816.

(36) Salamone, M.; Mangiacapra, L.; Bietti, M. *J. Org. Chem.* **2015**, *80*, 1149−1154.

(37) Milan, M.; Salamone, M.; Bietti, M. *J. Org. Chem.* **2014**, *79*, 5710−5716.

(38) The solvent's HBD ability can be conveniently expressed on the basis of Abraham's α_2^H parameter: α_2^H = 0.09 and 0.00 for MeCN and DMSO, respectively.[39]

(39) Abraham, M. H. *Chem. Soc. Rev.* **1993**, *22*, 73−83.

(40) (a) Rao, C. P.; Rao, M.; Rao, C. N. R. *Inorg. Chem.* **1984**, *23*, 2080−2085. (b) James, D. W.; Mayes, R. E. *J. Phys. Chem.* **1984**, *88*, 637−642. (c) Fussenegger, R.; Rode, B. M. *Chem. Phys. Lett.* **1976**, *44*, 95−99. (d) Balasubramanian, D.; Misra, B. C. *Biopolymers* **1975**, *14*, 1019−1026. (e) Balasubramanian, D.; Shaikh, R. *Biopolymers* **1973**, *12*, 1639−1650. (f) Balasubramanian, D.; Goel, A.; Rao, C. N. R. *Chem. Phys. Lett.* **1972**, *17*, 482−484. (g) Randall, E. W.; Yoder, C. M. S.; Zuckerman, J. J. *Inorg. Chem.* **1966**, *5*, 2240−2242. (h) Bull, W. E.; Madan, S. K.; Willis, J. E. *Inorg. Chem.* **1963**, *2*, 303−306.

(41) By increasing the concentration of $LiClO_4$ to 1.0 M, the upper limit to the rate constant for HAT from DMF can be lowered to $k_H <$ 5×10^3 M^{-1} s^{-1} (k_H(MeCN)/k_H(Li^+) > 260) as a consequence of the negligible effect on k_{obs} observed up to 2.0 M DMF.

(42) Izutsu, K. *Acid−Base Dissociation Constants in Dipolar Aprotic Solvents*; Blackwell: Oxford, 1990.

(43) Fukuzumi, S.; Ohkubo, K. *J. Am. Chem. Soc.* **2002**, *124*, 10270−10271.

(44) The following effective ionic radii are available for Li^+, Na^+, and Mg^{2+} with coordination number (CN) IV: 0.59, 0.99 and 0.57 Å, respectively; those for Li^+, Na^+, Mg^{2+}, and Ca^{2+} with CN VI are 0.76, 1.02, 0.72, and 1.00 Å, respectively.[45]

(45) Shannon, R. D. *Acta Crystallogr., Sect. A: Cryst. Phys., Diffr., Theor. Gen. Crystallogr.* **1976**, *32*, 751−767.

(46) For a critical discussion of the binding properties of Li^+ and Mg^{2+}, see: Dudev, T.; Lim, C. *J. Am. Chem. Soc.* **2011**, *133*, 9506−9515.

(47) Cabaleiro-Lago, E. M.; Ríos, M. A. *Chem. Phys.* **2000**, *254*, 11−23.

(48) (a) Peschke, M.; Blades, A. T.; Kebarle, P. *J. Am. Chem. Soc.* **2000**, *122*, 10440−10449. (b) Sajeevkumar, V. A.; Singh, S. *J. Mol. Struct.* **1996**, *382*, 101−110.

(49) See, for example: (a) Talukdar, D.; Borah, S.; Chaudhuri, M. K. *Tetrahedron Lett.* **2015**, *56*, 2555−2558. (b) Feng, J.; Lv, M. F.; Lu, G. P.; Cai, C. *Org. Chem. Front.* **2015**, *2*, 60−64. (c) Aruri, H.; Singh, U.; Sharma, S.; Gudup, S.; Bhogal, M.; Kumar, S.; Singh, D.; Gupta, V. K.; Kant, R.; Vishwakarma, R. A.; Singh, P. P. *J. Org. Chem.* **2015**, *80*, 1929−1936. (d) Sun, K.; Wang, X.; Li, G.; Zhu, Z.; Jiang, Y.; Xiao, B. *Chem. Commun.* **2014**, *50*, 12880−12883. (e) Majji, G.; Guin, S.; Rout, S. K.; Behera, A.; Patel, B. K. *Chem. Commun.* **2014**, *50*, 12193−12196. (f) Dian, L.; Wang, S.; Zhang-Negrerie, D.; Du, Y.; Zhao, K. *Chem. Commun.* **2014**, *50*, 11738−11741. (g) Yan, Y.; Zhang, Y.; Zha, Z.; Wang, Z. *Org. Lett.* **2013**, *15*, 2274−2277. (h) Takasu, N.; Oisaki, K.; Kanai, M. *Org. Lett.* **2013**, *15*, 1918−1921. (i) Boess, E.; Schmitz, C.; Klussmann, M. *J. Am. Chem. Soc.* **2012**, *134*, 5317−5325.